https://doi.org/10.5194/acp-2022-352
Preprint. Discussion started: 8 November 2022

Atmospheric Chemistry and Physics Discussions

Antarctic atmospheric Richardson number from radiosoundings measurements and AMPS

Qike Yang[1,2,3], Xiaoqing Wu[1,3], Xiaodan Hu[1,2,3], Zhiyuan Wang[1,3], Chun Qing[1,3], Tao Luo[1,3], Pengfei Wu[1,3], Yiming Guo[1,2,3]

[1]Key Laboratory of Atmospheric Optics, Anhui Institute of Optics and Fine Mechanics, HFIPS, Chinese Academy of Sciences, Hefei 230031, China
[2]Science Island Branch of Graduate School, University of Science and Technology of China, Hefei 230026, China
[3]Advanced Laser Technology Laboratory of Anhui Province, Hefei 230037, China

Correspondence to: Xiaoqing Wu (xqwu@aiofm.ac.cn)

Abstract. Monitoring a wide range of atmospheric turbulence over the Antarctic continent is still tricky, while the atmospheric Richardson number (Ri ; a critical parameter determining the possibility of turbulence could be triggered) is easier to obtain. The Antarctic atmospheric Ri , calculated using the temperature and wind speed, was investigated using the daily results from the radiosoundings and forecasts of the Antarctic Mesoscale Prediction System (AMPS). Radiosoundings for a year at three sites (McMurdo, South Pole, and Dome C) were used to quantify the reliability of the AMPS forecasts. The AMPS-forecasted $1/Ri$ (inverse of the Richardson number) can identify the main characteristics of atmospheric turbulence over the Antarctic continent in terms of space and time. The correlation coefficients (R_{xy}) of $1/Ri$ at McMurdo, South Pole, and Dome C are 0.71, 0.66, and 0.68, respectively, where the performance gains during the warm seasons. In addition, a model to improve AMPS-forecasted $1/Ri$ has been presented. The monthly median at the three sites and the seasonal median throughout the two vertical cross-sections for the AMPS forecasts are presented. One can observe that the probability of triggering turbulence is primarily concentrated near the ground. In addition, strong wind shears near escarpment regions have been found in the range of 0-5 km above the ground, thus causing atmospheric instability (or a thick boundary layer). In addition, turbulent atmospheres are likely to be triggered over the ocean, moving toward the Antarctic Plateau and becoming stable. Finally, the $1/Ri$ at the planetary boundary layer height ($PBLH$), $1/Ri_{PBLH}$, has been provided as a reference standard for judging atmospheric stability. The median value of $1/Ri_{PBLH}$ from the combined data of two vertical cross-sections was 0.55, which was used to calculate $PBLH$ and agree well with the AMPS forecasts (R_{xy} >0.72).

https://doi.org/10.5194/acp-2022-352
Preprint. Discussion started: 8 November 2022

Atmospheric Chemistry and Physics Discussions

1 Introduction

The Richardson number (Ri) is a valuable parameter for atmospheric stability monitoring; it combines both thermodynamic and dynamic profiles (Obukhov, 1971; Chan, 2008), which provides us with valuable insights into turbulent heat fluxes (Town and Walden, 2009) and the probability that optical turbulence (Yang et al., 2021b) can be triggered in Antarctica. However, measurements of atmospheric properties in Antarctica are sparse compared to those in the mid-latitudes and tropics. Atmospheric models have been developed to overcome this limitation (ECMWF by Geissler and Masciadri, 2006; Meso-NH by Lascaux et al., 2009; Polar WRF by Bromwich et al., 2013; MAR by Gallée et al., 2015), allowing researchers to investigate atmospheric variability beyond observational coverage, even for forecasting atmospheric properties in the future.

The Antarctic Mesoscale Prediction System (AMPS; https://www2.mmm.ucar.edu/rt/amps/) runs a real-time atmospheric model and provides numerical forecasts of Antarctica. The atmospheric model employed for AMPS is a Polar version of the Weather Research and Forecasting (Polar WRF) model (Powers et al., 2003). Polar WRF has been modified for use in polar regions, for example, improving the representation of heat transfer through snow and ice (Hines and Bromwich, 2008; Hines et al., 2015). The Polar WRF model was developed and maintained by the Polar Meteorology Group of the Byrd Polar and Climate Research Center (http://polarmet.osu.edu/PWRF/). The simulated Ri by Polar WRF seems to be reasonable in Antarctica when compared to an atmosphere-turbulence parameter (e.g., astronomical seeing by Yang et al., 2021b). In addition, various verification studies of the AMPS have been conducted (Seefeldt et al., 2011; Vázquez B and Grejner-Brzezinska, 2012; Wille et al., 2016; Listowski and Lachlan-Cope, 2017). However, previous verification studies have concentrated on and around the Ross Ice Shelf (or just a part of Antarctica), which needs to be extended.

And so far, monitoring a wide range of atmospheric turbulence over the Antarctic continent is still tremendous difficult at present, while the atmospheric Richardson number (Ri ; a critical parameter judging the possibility of the turbulence could be triggered) is easier to obtain, as it can be calculated by the routine meteorological parameters (temperature and wind speed). However, a precise evaluation of atmospheric models to forecast atmospheric Ri in Antarctica is sketchy. Nevertheless, the analyses from the European Centre for Medium-Range Weather Forecasts (ECMWF) have been used to calculate atmospheric $1/Ri$ (the inverse of the Richardson number) by Geissler and Masciadri (2006) and Hagelin et al. (2008). However, their researches have some specific shortages (or problems that need further study): (1) A direct comparison of $1/Ri$ between the model estimations and measurements has not been conducted. (2) Evaluations of forecast ability have not been done yet, while the forecast function is of great significance for practical application. (3) Variability of Ri at high horizontal spatial resolution has not been given, as previous studies focus on atmospheric profiles at separate sites. (4) A reasonable reference standard for judging the atmospheric stability by the model estimations was not given. To fill these gaps, the scientific goals of this paper are thus as follows.

https://doi.org/10.5194/acp-2022-352
Preprint. Discussion started: 8 November 2022


Atmospheric Chemistry and Physics Discussions

1. To carry out a detailed comparison of the temperature and wind speed (on which $1/Ri$ depends) in the atmospheric column, this study extends the evaluations performed by (Hagelin et al., 2008) above two sites to three sites (McMurdo, South Pole, and Dome C) over the Antarctic continent for a year. The three sites are considered representative, as the coast (McMurdo), flank (South Pole), and summit (Dome C) of the Antarctic continent will be compared using radiosoundings and AMPS forecasts.

2. Using the AMPS-forecasted meteorological parameters, we obtain the AMPS-forecasted $1/Ri$. The measured $1/Ri$ will also be calculated using the radiosounding-measured meteorological parameters. Then, a direct comparison between measurements and forecasts can be achieved, allowing us to evaluate the ability of the AMPS to forecast atmospheric stability or instability. In addition, we investigate how to correct the AMPS-forecasted $1/Ri$ and obtain a result closer to the measurements.

3. We also extended the analysis of $1/Ri$ done by (Hagelin et al., 2008) for three sites to two vertical cross-sections at a high horizontal resolution. Finally, regions and periods that are favourable for triggering atmospheric turbulence (or instability) can be identified. Thus, this study provides a better perspective on atmospheric dynamics in Antarctica.

4. To demonstrate the practicality of the AMPS-forecasted Ri and provide more information about the atmospheric properties over the Antarctic continent, the planetary boundary layer (PBL) height, $PBLH$, forecasted by the AMPS, is used to compare with the AMPS-forecasted $1/Ri$. $PBLH$ can be estimated where $1/Ri$ decreases to a critical value (e.g. Pietroni et al., 2011), denoted by $1/Ri_{PBLH}$. Then, $1/Ri_{PBLH}$ (i.e. $1/Ri$ at the PBL height) was obtained as a reference standard for judging whether the atmosphere was stable ($1/Ri < 1/Ri_{PBLH}$) or unstable ($1/Ri > 1/Ri_{PBLH}$) when using AMPS-forecasted $1/Ri$.

In Sect. 2, we present the experimental data and atmospheric model used in this study, with an explanation of their main characteristics. In Sect. 3, the Richardson number is introduced. In Sect. 4, we compare AMPS forecasts to radiosoundings and analyse the atmospheric properties in Antarctica. Sect. 5 discusses the relationship between the $1/Ri$ distribution and typical atmospheric features in Antarctica. Sect. 6 summarises the main aspects of this study.

2 Data and model

2.1 Radiosoundings

Daily radiosounding measurements at McMurdo (MM) and South Pole (SP) are available at the Antarctic Meteorological Research Center (AMRC; ftp://amrc.ssec.wisc.edu/pub). For Dome C (DC), one can access the measurements at the Antarctic Meteo-Climatological Observatory (http://www.climantartide.it). The altitudes of the three sites are 9 m (MM), 2839 m (SP), and 3239 m (DC), where the altitudes correspond to the height of the radiosoundings at the time of launch. Their locations are shown in Fig. 1. The radiosounding-measured meteorological parameters include pressure, temperature,

https://doi.org/10.5194/acp-2022-352
Preprint. Discussion started: 8 November 2022

Atmospheric Chemistry and Physics Discussions

wind speed, and wind direction. This study used one year of data (from March 2021 to February 2022). The radiosonde instrumentation used during this measurement period was the Vaisala RS41 (Technical data: https://www.vaisala.com/en/products/weather-environmental-sensors/upper-air-radiosondes-rs41). The accuracy and uncertainty of the radiosounding measurements are listed in Table 1. The balloon scans the atmosphere between the ground and an altitude of 10–25 km (low in winter and high in summer); the vertical resolution is approximately 5 m, depending on the ascent speed.

Table 1. Main technical specifications of the radiosonde instrumentation.

Measuring element	System resolution	System uncertainty	Data resolution[a]
Temperature	0.01 °C	0.15 °C (> 100 hPa)	0.1 °C
		0.30 °C (<100 hPa)	
Pressure	0.01 hPa	0.5 hPa (> 100 hPa)	0.1 hPa
		0.3 hPa (3-100 hPa)	
Wind speed	0.1 m/s	0.15 m/s	0.1 m/s (McMurdo)
			0.1 kts (South Pole)
			0.1 m/s (Dome C)
Wind Direction	0.1 deg	2 deg	0.1 deg (McMurdo)
			1 deg (South Pole)
			1 deg (Dome C)

[a] Resolution in the files that are available for download from the Web.

2.2 AMPS

The AMPS can forecast meteorological parameters in four-dimensional space-time in Antarctica, which can be used for comparison with the measurements of radiosoundings. The AMPS grid system consisted of a series of nested domains with 60 vertical levels. This study used grid 2 fields (d02; 8 km horizontal resolution) that covered the Antarctic continent (similar to Hines et al., 2019), as shown by the white square in Fig. 1. However, the contributions from the nested grid with higher horizontal resolution (d03: 2.67 km; d05: 0.89 km; d06: 2.67 km) are not entirely lost, as the AMPS used a two-way nested run and the nest (e.g. d03) feeds its calculation back to the coarser domain (e.g. d02). The original WRF output files for each grid were saved in a rolling archive (one can find how to access the original WRF output files of AMPS for each grid at https://www2.mmm.ucar.edu/rt/amps/information/amps_esg_data_info.html). This study used the AMPS outputs (in original WRF format) for forecast hours 12-21 at three h intervals from the daily AMPS forecasts that began at 12:00 UTC. Thus, our AMPS fields had a spin-up time of 12 h (similar to Hines and Bromwich, 2008; Hines et al., 2019). Finally, the AMPS forecasts for the same period (from March 2021 to February 2022), as the used radiosounding measurements, were downloaded for analysis.

https://doi.org/10.5194/acp-2022-352
Preprint. Discussion started: 8 November 2022

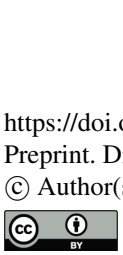

Atmospheric Chemistry and Physics Discussions

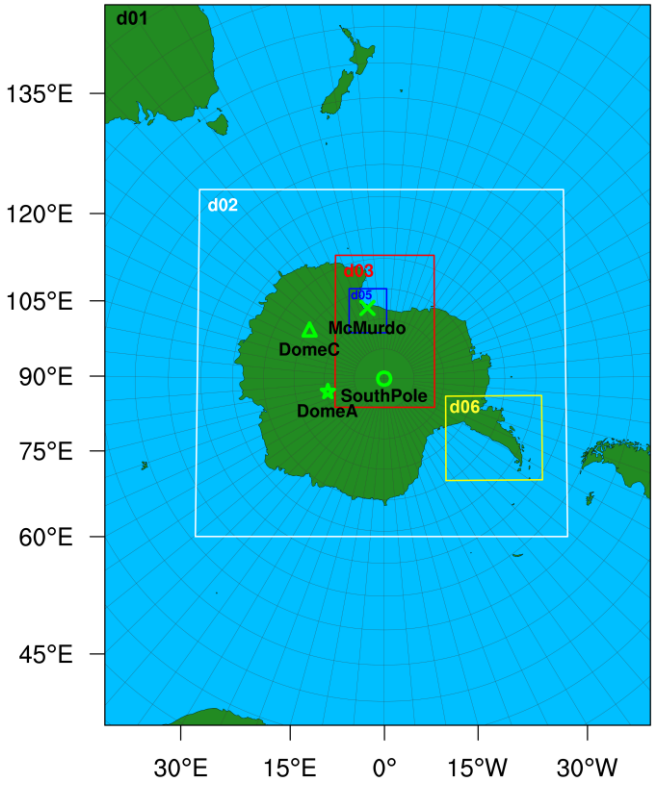

Figure 1. The five two-way interactive horizontal grids (d01, d02, d03, d05, and d06; information online at https://www2.mmm.ucar.edu/rt/amps/information/configuration/maps_2017101012/maps.html) used in the AMPS configuration. The locations of McMurdo (78°S, 167°E), South Pole (90°S, …°E), Dome C (75°S, 123°E), and Dome A (80°S, 78°E) are shown by the cross, circle, triangle, and star, respectively.

3 Theory of Richardson number

The stability of the atmosphere can be estimated using the Richardson number (Ri) (Obukhov, 1971; Chan, 2008):

$$Ri = \frac{g}{\theta} \frac{\partial\theta/\partial z}{\left[\partial u/\partial z\right]^2 + \left[\partial v/\partial z\right]^2}, \quad (1)$$

where g is the gravitational acceleration (9.8 m s^{-2}), $\theta = T\left[1000/P\right]^{0.286}$ is the potential temperature (K), T and P is the temperature (K) and pressure (hPa) of air, respectively. u and v are the east-west and north-south components of the wind (m s^{-1}).

The production of atmospheric turbulence (or unstable atmosphere) was shown to be tightly correlated with the Ri. It can, therefore, be an essential indicator of the turbulence characteristics in the atmosphere (Ma et al., 2020; Han et al., 2021; Yang et al., 2021b). Atmospheric conditions are favourable for the occurrence of turbulence when Ri is less than a critical

https://doi.org/10.5194/acp-2022-352
Preprint. Discussion started: 8 November 2022


Atmospheric Chemistry and Physics Discussions

value (Ri_c ; critical Richardson number). Ri_c is typically chosen as 0.25; however, a larger Ri_c should be used in a large-
125 scale model (e.g., 0.5 was employed by Troen and Mahrt, 1986).

In this study, the inverse of the Richardson number ($1/Ri$) was used to provide better evidence of atmospheric stability, as in Geissler and Masciadri (2006) and Hagelin et al. (2008). The larger the $1/Ri$, the higher the probability of triggering turbulence in the atmosphere.

4 Results

130 ### 4.1 Temperature and wind speed

The AMPS forecasts are compared to radiosoundings from MM, SP, and DC to investigate the reliability of the AMPS forecasts over the Antarctic continent. The AMPS forecasts and radiosoundings used for this comparison were obtained from March 2021 to February 2022. To offer a more convincing result, data corresponding to the altitude at which radiosoundings reached less than five times a month were discarded. In addition, the extracted AMPS forecasts used for comparison were
135 from the nearest grid to the three sites, and the time difference between AMPS forecasts and radiosoundings larger than 1.5 hours was also not used for comparison. Moreover, both AMPS forecasts and radiosoundings were linearly interpolated to the same height series (average annual altitude of the AMPS vertical grid, because the altitude of the AMPS grid may vary during the simulation as the AMPS uses the hybrid vertical coordinate, information online at https://www2.mmm.ucar.edu/wrf/users/docs/user_guide_v4/WRFUsersGuide.pdf) for each site.

140 The monthly medians of the temperature differences (Fig. 2) and wind speed (Fig. 3) between the AMPS forecasts and radiosoundings are presented. The panels in the same row of Figs. 2 and 3 correspond to the same season; the first row: Aut. (Autumn: March, April, and May), second row: Win. (Winter: June, July, and August), third row: Spr. (Spring: September, October, and November), fourth row: Sum. (Summer: December, January, and February). The missing value of the median difference in the upper part of the atmosphere indicates that the radiosoundings do not reach as high an AGL (Above Ground
145 Level) in winter as they do in summer, probably because the elastic material of the balloons is more fragile in cold seasons and easier to explode (Hagelin et al., 2008). The lack of measurements may also be attributable to some large values of the median difference in the top layer of the profile shown in Figs. 2 and 3.

https://doi.org/10.5194/acp-2022-352
Preprint. Discussion started: 8 November 2022

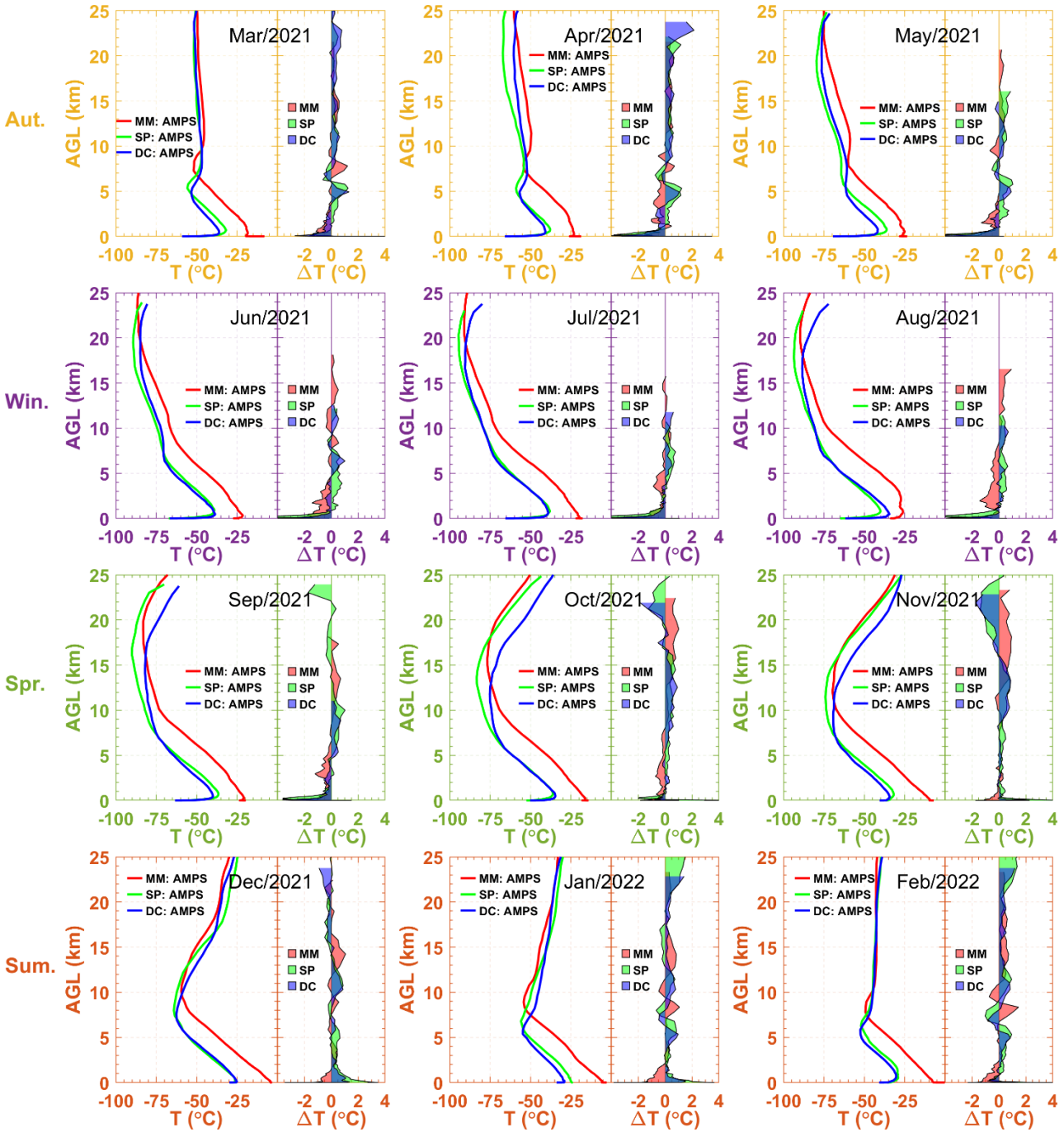

Figure 2. The monthly median for temperature forecasted by the AMPS (solid lines) and temperature difference calculated by the AMPS forecasts minus the radiosoundings measurements, i.e. $\Delta T = T_{AMPS} - T_{Mea.}$ (filled areas).

https://doi.org/10.5194/acp-2022-352
Preprint. Discussion started: 8 November 2022

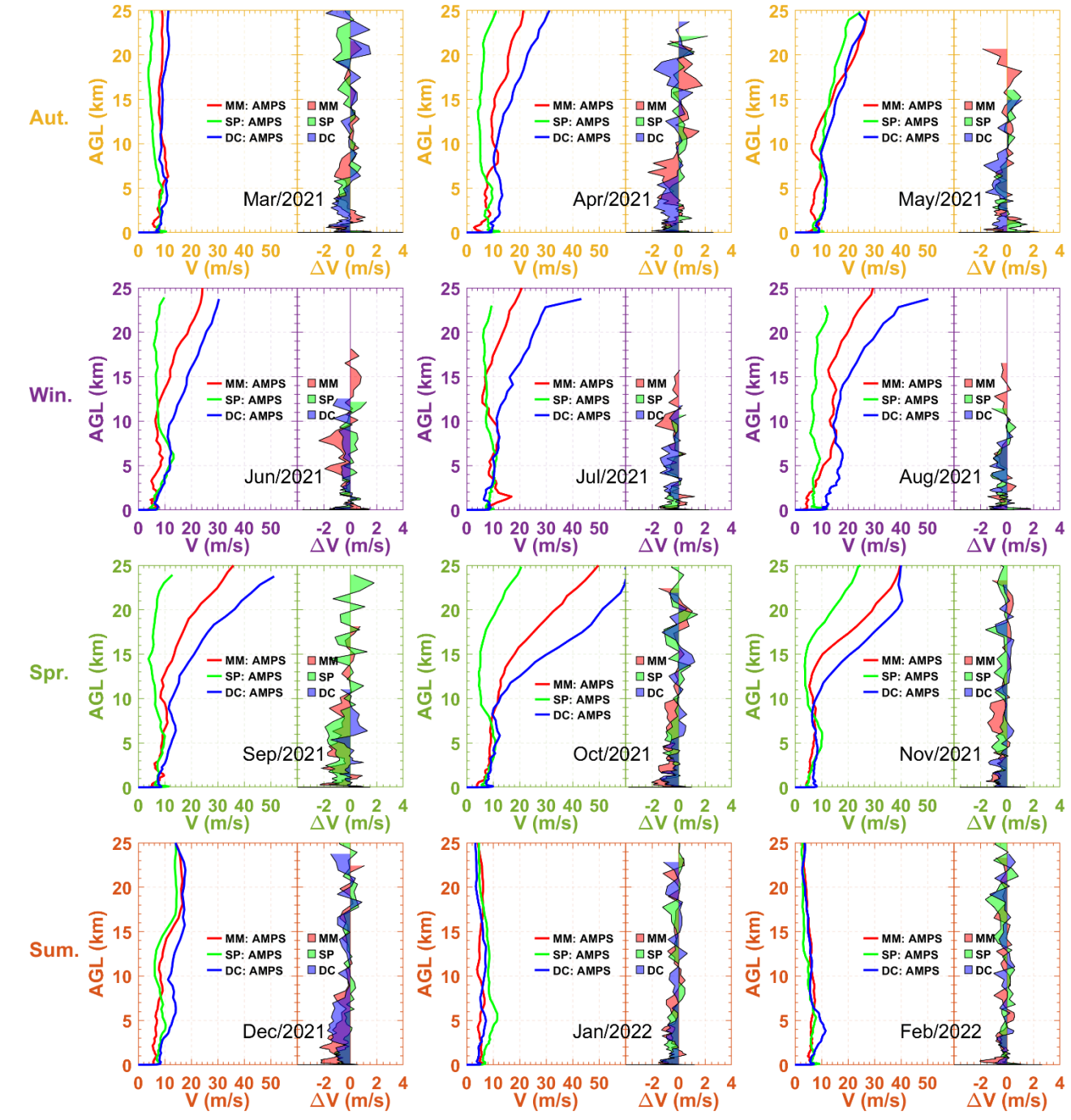

Figure 3. As in Fig 2, but for wind speed V ($=\sqrt{u^2+v^2}$), and $\Delta V = V_{AMPS} - V_{Mea.}$.

https://doi.org/10.5194/acp-2022-352
Preprint. Discussion started: 8 November 2022


Atmospheric Chemistry and Physics Discussions

Fig. 2 shows that the forecasted temperature profiles of SP and DC in the first 5 km are similar, 15-20 K colder than the MM. The median difference in the temperature is of the order of 1 K in the high part of the atmosphere (see filled areas in Fig. 2). However, in proximity to the ground, the median difference becomes more significant, especially for winter (similar to Bromwich et al., 2013), at more than 4 K near the ground at SP.

Fig. 3 shows that the forecasted wind speed profiles of MM and DC above 10 km are stronger during spring, indicating the occurrence of the Antarctic polar vortex (Boville et al., 1988). However, the change in wind speed above SP is not that obvious, because the Antarctic vortex is roughly pole-centred (Karpetchko et al., 2005). From the filled areas in Fig. 3, the AMPS forecasts appear consistent with the measurements, as the median difference in wind speed is generally ~1 m s^{-1} and has barely exceeded 2 m s^{-1}, whether the wind is strong or weak. In addition, slightly smaller median differences were displayed around 10 km AGL (e.g. September and December, shown in Fig. 3), and the forecasted wind speed also became slightly smaller at that height.

In summary, the AMPS almost well forecasted the temperature and wind speed. Nevertheless, it should be noted that both the measurement accuracy and position of radiosoundings may be affected by their flight, and the difference may be smaller when compared with a fixed measuring instrument, such as the Automatic Weather Station (Hagelin et al., 2008). In other words, the functional performance of the AMPS may be better than the results shown in Figs. 2 and 3.

4.2 Richardson number

4.2.1 Monthly statistical analysis

To evaluate the performance of the AMPS in forecasting atmospheric stability or instability over the Antarctic continent, the $1/Ri$ forecasted by AMPS and measured by radiosoundings will be provided. The calculated value of $1/Ri$ depends on the vertical resolution of meteorological parameters (Troen and Mahrt, 1986; Holtslag et al., 1990). Thus, the meteorological parameters from the AMPS forecasts and radiosoundings were interpolated into the same height series (as mentioned in Sect. 4.1) to calculate $1/Ri$.

https://doi.org/10.5194/acp-2022-352
Preprint. Discussion started: 8 November 2022

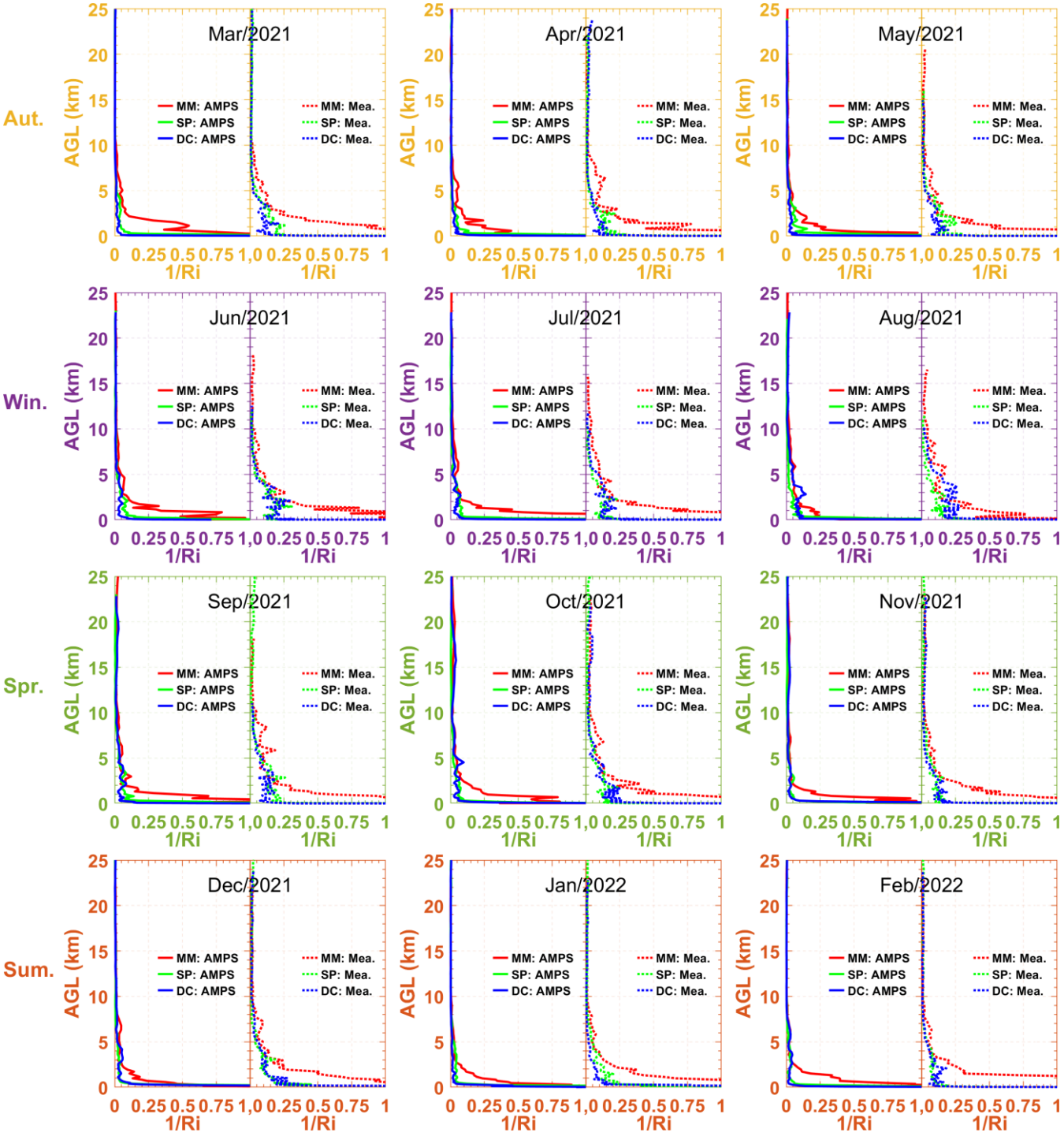

Figure 4. The monthly median for $1/Ri$ forecasted by the AMPS (solid lines) and measured by radiosoundings (dashed lines).

https://doi.org/10.5194/acp-2022-352
Preprint. Discussion started: 8 November 2022


Atmospheric Chemistry and Physics Discussions

The NCL (NCAR Command Language) can compute Ri from the original WRF outputs, using an NCL function called "rigrad_bruntv_atm" (http://www.ncl.ucar.edu/Document/Functions/Contributed/rigrad_bruntv_atm.shtml). The NCL-computed Ri (not shown) agrees very well with the results obtained using interpolation (i.e. interpolating the hybrid vertical coordinate to the same height series for each site).

The monthly median profiles of $1/Ri$ from the AMPS and radiosoundings are shown in Fig. 4. However, the median differences are not similar to those of the previous temperature and wind speed. This is because, the value of $1/Ri$ can oscillate massively in the atmosphere, and precise quantification seems less plausible. Nevertheless, the AMPS-forecasted Ri can identify that the atmosphere above MM tends to be more unstable (or turbulent, $1/Ri$ is large) than SP and DC, per the measurements from radiosoundings. In addition, in the vertical height direction, AMPS forecasts can roughly capture the height that can easily trigger turbulence. On the one hand, one can observe that $1/Ri$ from AMPS forecasts and radiosoundings both show large values very close to the ground at Dome C and the South Pole, which is per the fact that strong atmospheric turbulence is concentrated within the surface layer (Marks et al., 1999; Aristidi et al., 2005; Agabi et al., 2006). A very calm atmosphere ($1/Ri$ is small) at high altitudes was also indicated by Travouillon et al. (2003), Trinquet et al. (2008) and Vernin et al. (2009). On the other hand, in a more detailed comparison, for example, in March 2021, both forecasts and measurements show that $1/Ri$ profiles are inclined to the y-axis at ~10 km AGL, and in December 2021, the AMPS forecasts are able to capture a small bump of $1/Ri$ that occurred at around 7 km AGL.

Some researchers are afraid to conduct quantitative analysis for the model-estimated $1/Ri$ as it always varies dramatically (Hagelin et al., 2008). Nevertheless, quantitative analysis has been tried in this study since that can give a precise evaluation of the forecast ability of AMPS. Then, the correlation coefficient (R_{xy}), mean bias ($Bias$; AMPS-radiosoundings), and root mean square error ($RMSE$) are calculated. Here, the time difference between AMPS forecasts and radiosoundings, with lesser than 1.5 hours, is used. This is the same as the meteorological parameters mentioned in Sect. 4.1. Besides, all profile data meeting the time constraints are also limited to a value range of (0, 1), which is the same as the x-axis in Fig. 4. Finally, the monthly values of the three statistical operators are obtained, as shown in Fig. 5. However, we want to emphasise that one should focus on the value of R_{xy} that reflects the tendency, instead of $Bias$ and $RMSE$, as precise quantification remains in doubt (Hagelin et al., 2008). The mean values of the combined 12 monthly R_{xy} in Fig. 5a for MM, SP, and DC, are 0.71, 0.66, and 0.68, respectively. This suggests that the AMPS-forecasted $1/Ri$ can identify the main characteristics of atmospheric turbulence over the Antarctic continent in terms of space and time. In terms of time, one can observe larger R_{xy} during warm seasons (e.g. Autumn from March 2021 to May 2021 and summer from December 2021 to February 2022). In sum, the AMPS seems to perform better when more measurements can be obtained. As we know, more field experiments could be conducted at the coast (MM) in the space dimension (one can reach the coast easier than the internal Antarctic

https://doi.org/10.5194/acp-2022-352
Preprint. Discussion started: 8 November 2022

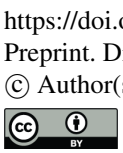

Atmospheric Chemistry and Physics Discussions

Plateau) and during warm seasons (e.g., summer) in the time dimension (the cold is much harder to endure in winter than it is in summer).

Fig. 5b shows that $1/Ri$ is underestimated every season, and the mean values of the 12 monthly *Bias* for MM, SP, and DC are -0.097, -0.031, and -0.071, respectively. This may be because the model results were generally smoother than the measurements. The atmosphere is favourable for the occurrence of turbulence ($1/Ri$ is large) under rapidly changing meteorological parameters. Fig. 5c shows that *RMSE* at MM is the largest, which may be due to the relatively unstable atmosphere above it and $1/Ri$ could fluctuate massively.

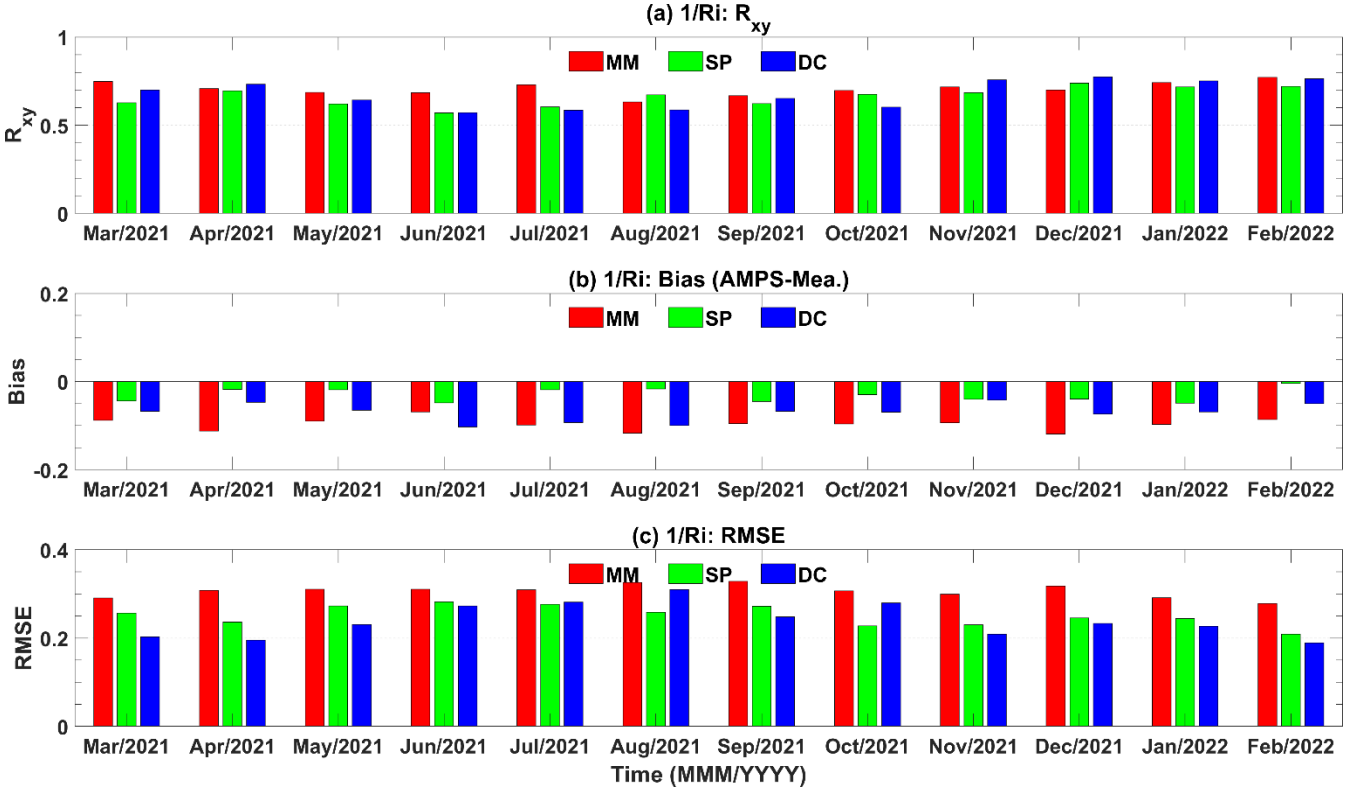

Figure 5. The monthly $1/Ri$ statistics for three sites.

4.2.2 Vertical distribution

To further investigate the difference between the radiosounding and model results, the vertical distributions of the whole-year $\log_{10}(1/Ri)$ at the three sites are shown in Fig. 6. The reason for using $\log_{10}(1/Ri)$ (not $1/Ri$, as presented in Sect. 4.2.1) is that we find that the distribution will be more linear at the same height. Fig. 6a shows that the data points are distributed mainly over the diagonal line between the measurements and the forecasts, this suggests the AMPS can make a better forecast $\log_{10}(1/Ri)$ at McMurdo than at the South Pole (Fig. 6b) and Dome C (Fig. 6c).

https://doi.org/10.5194/acp-2022-352
Preprint. Discussion started: 8 November 2022

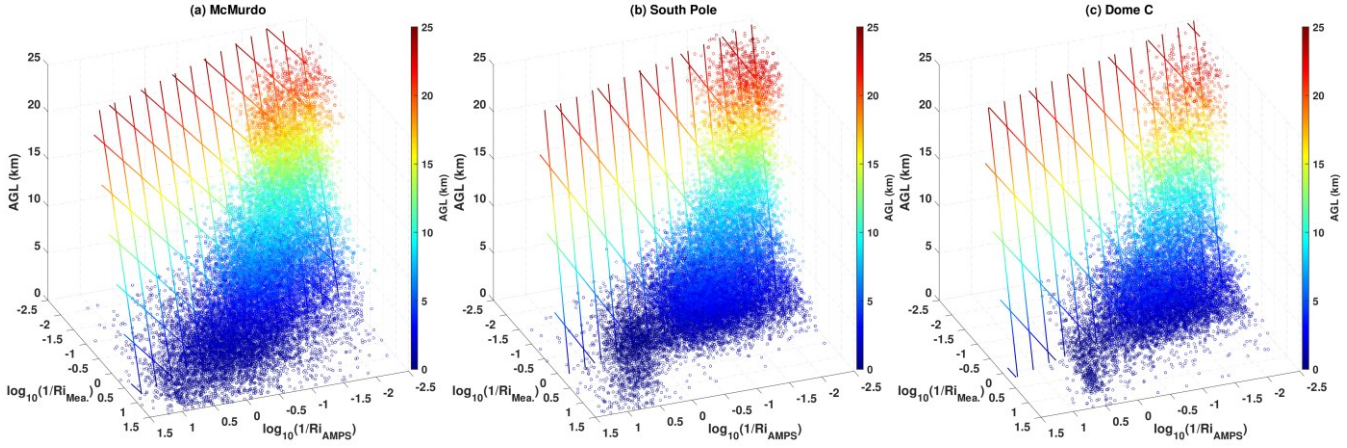

Figure 6. the vertical distributions of whole-year $\log_{10}(1/Ri)$ from the AMPS and the measurements at McMurdo (a), the South Pole (b), and Dome C (c). The coloured grid lines represent the fitted planes using the presented data points.

We assume that the difference between the measurements and model results was correlated with height (or AGL, here indicated by H), and a simple model to improve the AMPS-forecasted $1/Ri$ by considering H (km) is given by the following linear equation:

$$\log_{10}\left(1/Ri_{\text{ImpAMPS}}\right) = C_1 + C_2 \cdot \log_{10}\left(1/Ri_{\text{AMPS}}\right) + C_3 \cdot H \,. \tag{2}$$

The three undetermined coefficients (C_1, C_2, and C_3) can be determined using a linear fitting by the measurements, $1/Ri_{\text{Mea.}}$ (i.e. $1/Ri_{\text{ImpAMPS}}$ will be replaced with $1/Ri_{\text{Mea.}}$ for fitting).

Table 2. The fitted model for improving the AMPS-forecasted $1/Ri$.

Site	Model: $\log_{10}\left(1/Ri_{\text{ImpAMPS}}\right) = C_1 + C_2 \cdot \log_{10}\left(1/Ri_{\text{AMPS}}\right) + C_3 \cdot H$	R_{xy} (Before)[a]	R_{xy} (After)[b]
McMurdo	$\log_{10}\left(1/Ri_{\text{ImpAMPS}}\right) = 0.1222 + 0.4826 \cdot \log_{10}\left(1/Ri_{\text{AMPS}}\right) - 0.0660 \cdot H$	0.7215	0.7691
South Pole	$\log_{10}\left(1/Ri_{\text{ImpAMPS}}\right) = -0.4414 + 0.3827 \cdot \log_{10}\left(1/Ri_{\text{AMPS}}\right) - 0.0387 \cdot H$	0.6009	0.6391
Dome C	$\log_{10}\left(1/Ri_{\text{ImpAMPS}}\right) = -0.3596 + 0.3977 \cdot \log_{10}\left(1/Ri_{\text{AMPS}}\right) - 0.0457 \cdot H$	0.4730	0.5235

[a] Correlation coefficient between $\log_{10}\left(1/Ri_{\text{Mea.}}\right)$ and $\log_{10}\left(1/Ri_{\text{AMPS}}\right)$ (i.e. before using the fitted model).

[b] Correlation coefficient between $\log_{10}\left(1/Ri_{\text{Mea.}}\right)$ and $\log_{10}\left(1/Ri_{\text{ImpAMPS}}\right)$ (i.e. after using the fitted model).

https://doi.org/10.5194/acp-2022-352
Preprint. Discussion started: 8 November 2022

Atmospheric Chemistry and Physics Discussions

240 Table 2 lists the fitted model and its corresponding improvements. The correlation coefficient at all three sites increased after using the fitted model, which means that the fitted model can be used to modify the AMPS forecasts ($1/Ri_{\mathrm{AMPS}}$) and obtain an improved result ($1/Ri_{\mathrm{ImpAMPS}}$). Through analysis of the fitted model, one can see the undetermined coefficient C_2 is less than 1, we find this is due to the AMPS underestimated $\log_{10}(1/Ri)$ when $\log_{10}(1/Ri)$ <0; the undetermined coefficient C_3 is negative, indicating the negative regulating action for $1/Ri_{\mathrm{AMPS}}$ with increasing height.

245 **4.2.3 Vertical cross-section**

The results are given in Sect. 4.2.1 that shows the AMPS can forecast the main tendency of $1/Ri$. The analysis of $1/Ri$ was done through interpolation of the AMPS grid 2 field with two vertical cross-sections, which provides us with a broader perspective on the probability of turbulence triggered in four-dimensional space-time. One vertical cross-section is interpolated through two specified points (the South Pole and Dome C), and another is through Dome A and McMurdo (Fig.
250 7). The corresponding AMPS forecasts are shown in Fig. 8 and 9, respectively.

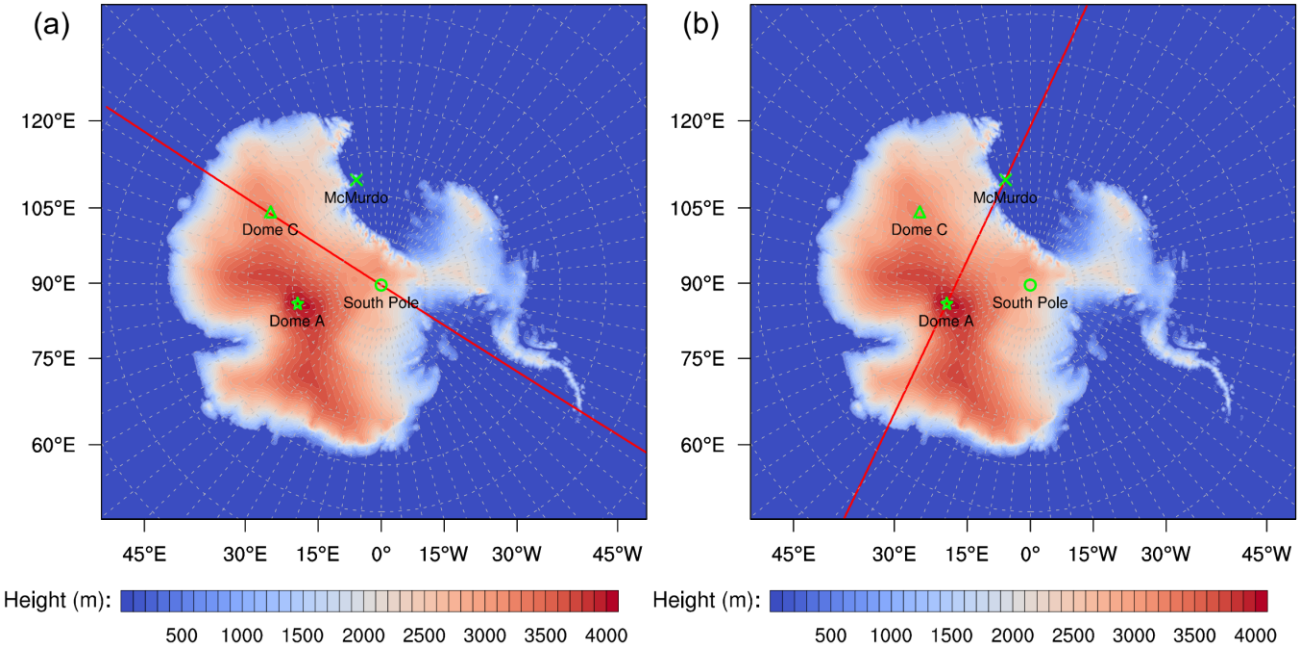

Figure 7. Two lines (red) are used to create vertical cross-sections. (a) a line through Dome C and the South Pole, (b) a line through Dome A and McMurdo. The colour scale indicates the terrain height (m).

255

https://doi.org/10.5194/acp-2022-352
Preprint. Discussion started: 8 November 2022

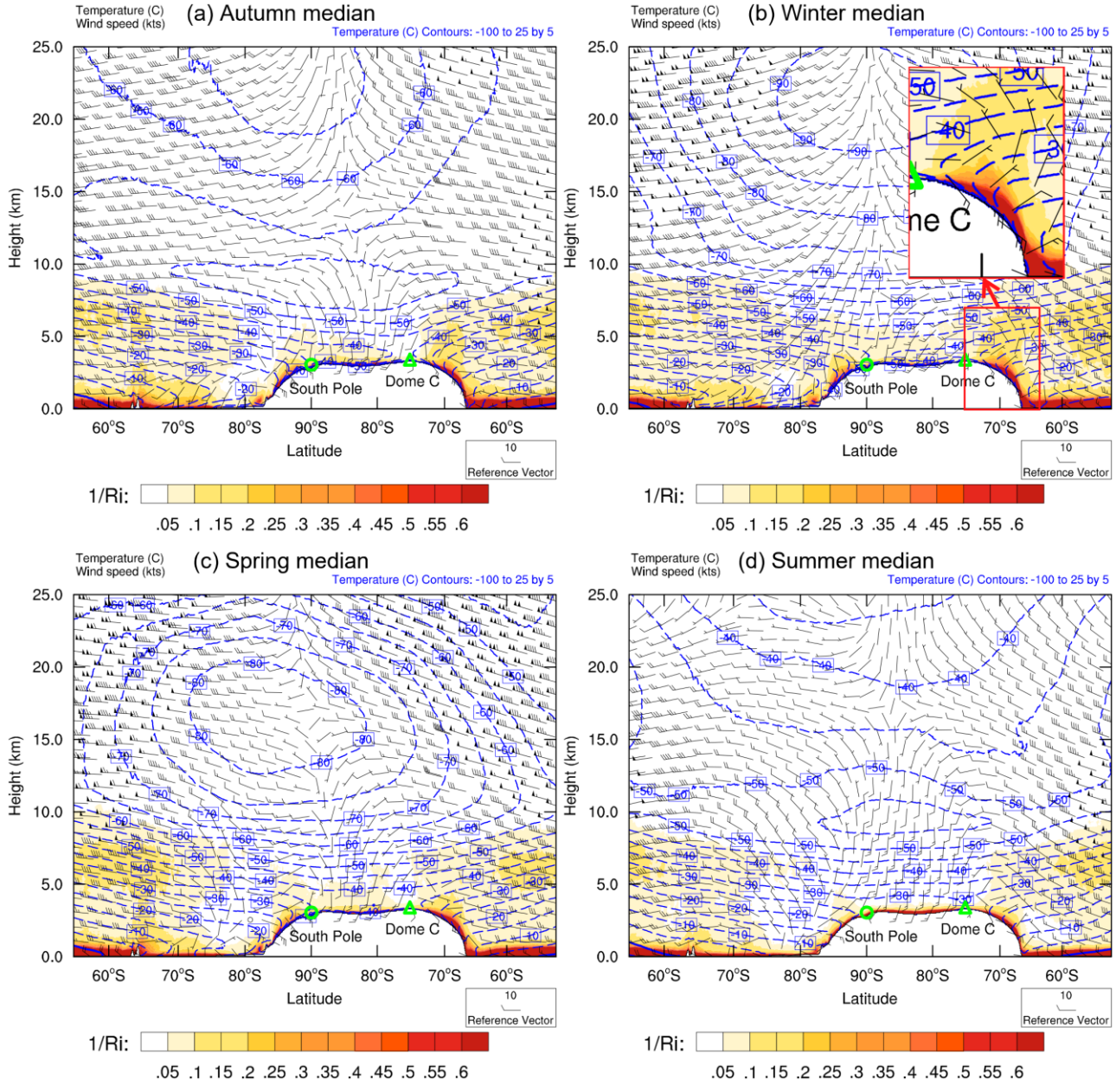

Figure 8. Median vertical cross-section of temperature, wind speed, and $1/Ri$ along the red line through the South Pole and Dome C (shown in Fig. 7a). The height (km) on the y-axis represents the elevation above sea level. The seasonal median for autumn: March 2021 to May 2021 (a), winter: June 2021 to August 2021 (b), spring: September 2021 to November 2021 (c), and summer: December 2021 to February 2022 (d) are given. The reference vector is 10 kts (~5.2 m s^{-1}) for the wind barb. Winds are depicted as blowing from the direction the flags are facing (earth coordinates), e.g., the reference vector represents wind blowing from the west.

https://doi.org/10.5194/acp-2022-352
Preprint. Discussion started: 8 November 2022

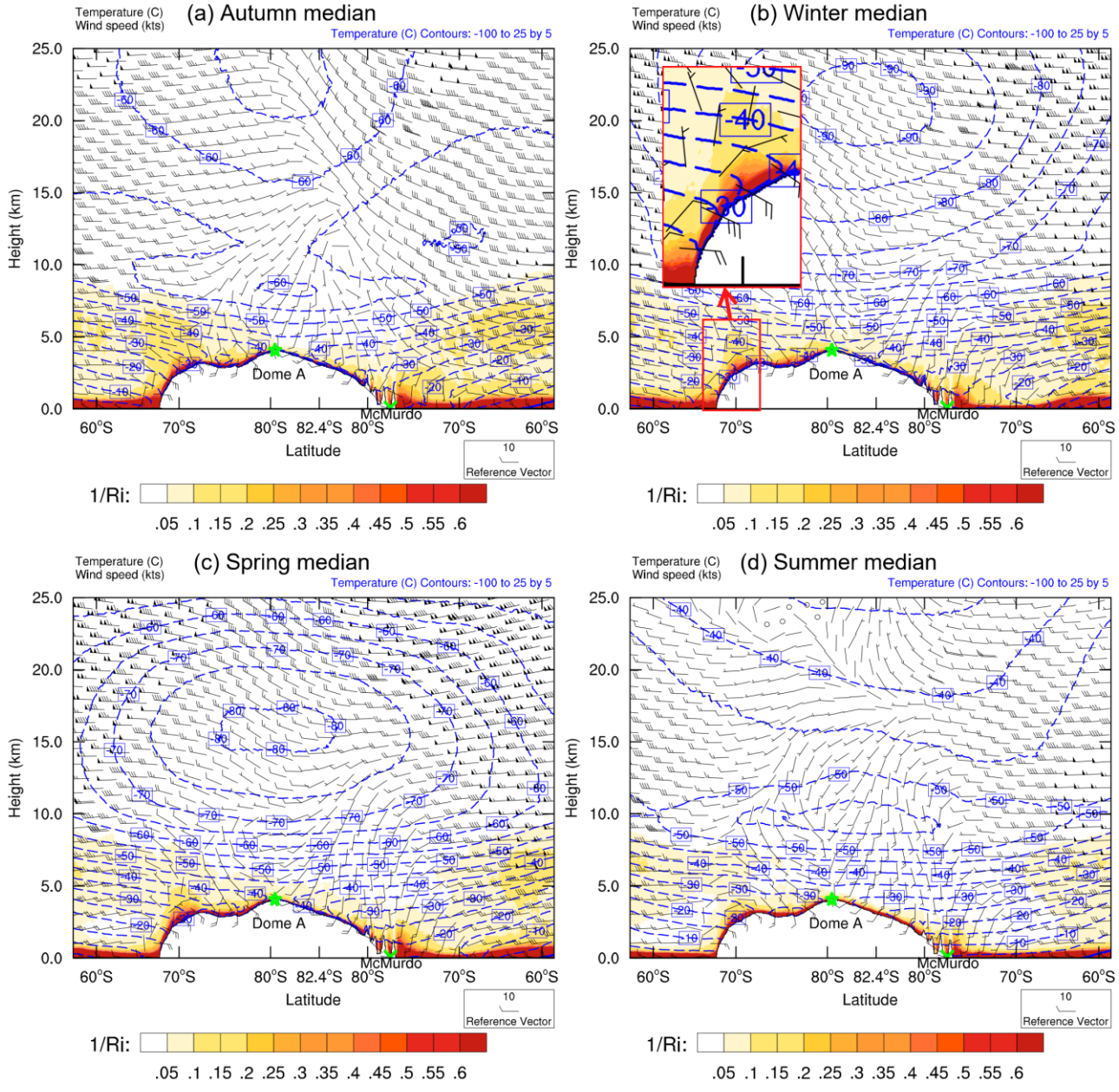

Figure 9. As in Fig. 8, but for the vertical section along the red line through Dome A and McMurdo (shown in Fig. 7b).

Figs. 8 and 9 show the seasonal median of the AMPS forecasts. The temperature and wind speed were lower above the Antarctic Plateau than over the ocean. In the polar winter, the temperature contours are dense near the ground above the interior Plateau, representing a strong surface-layer temperature inversion (similar to Yagüe et al., 2001; Argentini et al.,

https://doi.org/10.5194/acp-2022-352
Preprint. Discussion started: 8 November 2022


Atmospheric Chemistry and Physics Discussions

2013; Hu et al., 2019). The surface-layer wind speeds increase from the summit to the escarpment region (the well-known katabatic wind over the surface slope area in Antarctica) and then decrease toward the coast, which is consistent with previous measurements (Ma et al., 2010; Rinke et al., 2012). The depths of large $1/Ri$ near the ground are thinner near the summits (e.g. Dome A and Dome C) of the Antarctic Plateau (similar to Swain and Gallée, 2006; Bonner et al., 2010; Aristidi et al., 2015). Notably, a thick depth of large $1/Ri$ (which could be considered thick $PBLH$ and will be discussed later) occurred near the escarpment region from the side of the internal plateau, as clearly shown during winter (see the enlarged drawings in Figs. 8 and 9). Owing to the forecast ability of AMPS in vertical space, one can see that this high $PBLH$ is caused by the wind shear, where the wind direction is southeast within the surface layer (one can see similar results in the surface layer from Yang et al., 2021a) and changes to the northwest at ~ 5 km AGL.

In addition, one can see the temporal evolution of $1/Ri$ vertical cross-sections for a year from the video supplement (vertical cross-section through the red line shown in Fig. 7a: https://doi.org/10.5446/57377; Fig. 7b: https://doi.org/10.5446/57378). It shows that the atmosphere exhibited strong daily variability. Thus, forecasting $1/Ri$ is necessary if one wishes to avoid a turbulent atmosphere in Antarctica, instead of counting only on the displayed statistical results. Moreover, unstable atmospheres are likely to be triggered over the ocean, moving toward the Antarctic Plateau and becoming stable. This was likely due to the obstruction of the high plateau, and the atmosphere above it behaved calmly.

4.2.4 Richardson number at the planetary boundary layer height

The Richardson number is used to determine the boundary layer height using a critical value (Troen and Mahrt, 1986; Holtslag et al., 1990; Pietroni et al., 2011). The critical value (or the value of $1/Ri$ at the $PBLH$, $1/Ri_{PBLH}$) is worth studying, which is a significant application for the Richardson number. In addition, previous studies have suggested that the Richardson number depends on the vertical resolution of the model (Troen and Mahrt, 1986; Holtslag et al., 1990). It is difficult to define what strong turbulence layer (or atmosphere instability) may appear, whenever a reference standard is not given. $1/Ri_{PBLH}$ would thus be a helpful reference standard for judging whether an atmospheric layer is stable ($1/Ri < 1/Ri_{PBLH}$) or unstable ($1/Ri > 1/Ri_{PBLH}$).

The PBL scheme of the AMPS used the Mellor-Yamada-Janjić (MYJ; Janjić, 1994) scheme, and the ability of the AMPS to model the Antarctic PBL was examined by Wille et al. (2017). The MYJ scheme defines the $PBLH$ where turbulent kinetic energy decreases to a prescribed value of 0.1 m^2 s^2 (Xie et al., 2012), and the AMPS forecasts include the values of $PBLH$. Figs. 10a (DC) and 11b (DA) show that the $PBLH$ directly forecasted by the AMPS (red lines) was mostly less than 100 m during the polar winter, which is consistent with the SODAR observations (DC: Petenko et al., 2014; DA: Bonner et al., 2010); Fig. 10b also displays a result being in accordance with the SODAR observations at the SP, as $PBLH$ was shown to be within 100-300 m (Travouillon et al., 2003). Thus, the AMPS-forecasted $PBLH$ is considered believable. Figs. 10c and 11c show the median annual $PBLH$ along the red lines in Figs. 7a and 7b, respectively. One can observe that

https://doi.org/10.5194/acp-2022-352
Preprint. Discussion started: 8 November 2022

Atmospheric Chemistry and Physics Discussions

the AMPS-forecasted $PBLH$ is thin over the plateau, especially for the summits (e.g., Dome A and Dome C), which agrees with previous studies (Swain and Gallée, 2006). While thick $PBLH$ are shown near the escarpment region, as seen by the dump in ~67°S (up) in Fig. 10c and ~68°S (down) in Fig. 11c. This corresponds to the thick depth of the large $1/Ri$ shown in enlarged drawings (Figs. 8 and 9).

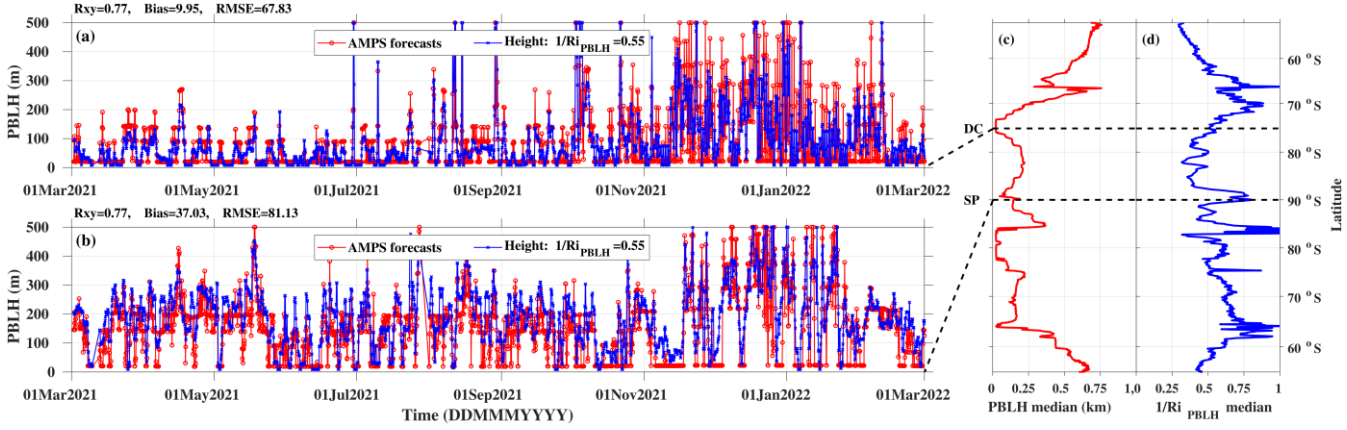

Figure 10. Temporal evolution of $PBLH$ directly forecasted by the AMPS (red circles) and estimated by the height corresponding to $1/Ri = 1/Ri_{PBLH} = 0.55$ (blue crosses) at DC (a) and SP (b). Median annual $PBLH$ (c) and $1/Ri_{PBLH}$ (d) along the red line through DC and SP shown in Fig. 7a.

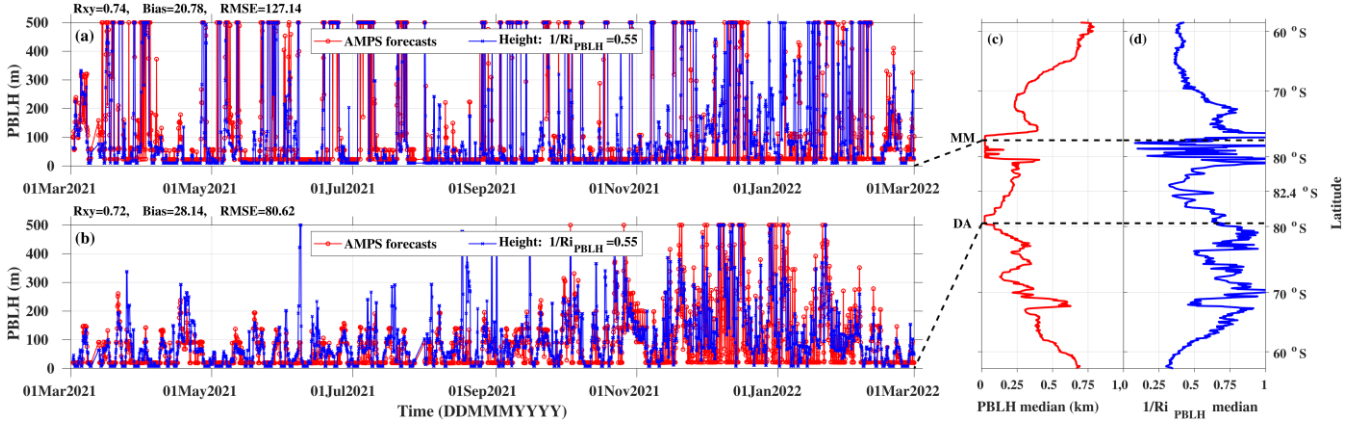

Figure 11. As in Fig. 10, but for data along the red line through MM and DA showed in Fig. 7b.

Then, $1/Ri_{PBLH}$ was computed using linear interpolation between the AMPS grid with height equals $PBLH$. The median value of $1/Ri_{PBLH}$ from the combined data of two vertical cross-sections was calculated as 0.55 to give only one typical value. However, some researchers have proposed $1/Ri_{PBLH}=4$ ($Ri_{PBLH}=0.25$) when radiosoundings with high vertical resolution are

https://doi.org/10.5194/acp-2022-352
Preprint. Discussion started: 8 November 2022


Atmospheric Chemistry and Physics Discussions

used (e.g. at Dome C; Pietroni et al., 2011). Here, the smaller critical value for the AMPS forecasts may be caused by the coarse vertical grid resolution of the AMPS (as indicated by Troen and Mahrt, 1986) and its data smoothness (as mentioned in Sect. 4.2.1; the AMPS forecasts show smaller $1/Ri$ than the radiosoundings that have already been interpolated to the vertical resolution as the AMPS).

To test the credibility of the critical value (i.e. $1/Ri_{PBLH}$ =0.55), $PBLH$ was also derived as the height where the AMPS-forecasted $1/Ri$ decreases to 0.55 (blue lines in Figs. 10a-b and 11a-b). Even if larger critical values are used, no substantial variations would occur in the estimate because of the large gradient of $1/Ri$ near the ground (Fig. 4), also mentioned in Pietroni et al. (2011). In the internal Antarctic Plateau (DC, SP, and DA), the $PBLH$ shows a slight change in magnitude during the cold seasons (e.g. from March to October 2021). Such seasonal variation is not significant along the coast of Antarctica (MM), which fluctuates every season. During the polar summer (e.g. January 2022) at all four sites, $PBLH$ estimated by $1/Ri_{PBLH}$ =0.55 and read directly from the AMPS forecasts fluctuate considerably. The R_{xy}, $Bias$, and $RMSE$ of $PBLH$ between the estimations using the critical value ($1/Ri_{PBLH}$ =0.55) and AMPS forecasts, are depicted in the top left of the plot. It appears that the values of R_{xy} (>0.72) are almost satisfactory, and we may conclude that 0.55 is a reliable critical value for judging the behaviour of atmospheric turbulence. The atmosphere layer could be considered turbulent when $1/Ri$ >0.55 (this may only be valid for using the AMPS forecasts). $Bias$ >9 indicates the results calculated by this critical value overestimate the $PBLH$. And $RMSE$ >67 suggests that one should be careful when estimating a precise value for $PBLH$ with this critical value (0.55).

5 Discussion

The above results of the $1/Ri$ distribution provided us with valuable insights into the atmospheric turbulence in the Antarctic region. Here, we attempt to relate the features of atmospheric turbulence to some typical atmospheric conditions in Antarctica: temperature inversion, katabatic winds, and polar vortices.

The strength of the near-ground temperature inversion increases from the coast to the interior of Antarctica, and its strength weakens during summer (Fig. 2), such a phenomenon has also been observed in previous studies (Hudson and Brandt, 2005; Ma et al., 2010). Combined with the analysis of Figs. 11 and 12, the general increase in temperature-inversion strength was found to correspond to a less turbulent atmosphere with smaller $1/Ri$ (when the boundary layer is thinner), owing to large stability suppressing turbulence.

As a result of typical katabatic winds (Rinke et al., 2012), the wind speeds increase from the interior plateau to the steep slope (Figs. 8 and 9). Strong winds can lead to increased levels of mechanical turbulence, as one can see a thick depth of large $1/Ri$ layer at the escarpment region.

https://doi.org/10.5194/acp-2022-352
Preprint. Discussion started: 8 November 2022


Atmospheric Chemistry and Physics Discussions

A strong polar vortex means that zonal winds are strong, and atmospheric turbulence is more likely to be triggered. The Antarctic polar vortex reaches its peak intensity in the winter-spring and weakens during summer (Zuev and Savelieva, 2019a). One can also see that the free atmosphere in Antarctica becomes relatively calm during summer, as shown by the smaller $1/Ri$ in Figs. 8d and 9d. On the other hand, the strongest zonal winds exist over the ocean (see the wind speed shown in Figs. 8 and 9, also in Zuev and Savelieva, 2019b), which suggests that the atmosphere above the ocean can be an important source of turbulence (Figs. 8 and 9 show larger $1/Ri$ over the ocean).

6 Conclusion

We examined the ability of AMPS to forecast the inverse of the Richardson number ($1/Ri$; the larger the $1/Ri$, the higher the probability of triggering turbulence in the atmosphere) in the Antarctic atmosphere. This includes quantifying the accuracy of meteorological parameters (Temperature and wind speed, on which the $1/Ri$ depends), and comparing the $1/Ri$ from the AMPS forecasts and radiosoundings. In addition, the analysis of atmospheric $1/Ri$ over the Antarctic continent and the ocean surrounding it, was presented on an annual time scale. Further, the $PBLH$ forecasted by the AMPS was employed to understand how to evaluate atmospheric stability or instability using the value of $1/Ri$.

From the analysis presented above, we deduce the following:

1. Comparisons of the AMPS forecasts with the radiosoundings from three representative sites (coast: McMurdo, flank: the South Pole, summit: Dome C) show that the forecasts can accurately describe the atmospheric meteorological parameters above the Antarctic continent in almost the whole range from the ground to 25 km AGL. The monthly median difference in the air temperature is of the order of 1 K in a large part of the atmosphere, where the cold temperature bias occurs near the ground during winter. As for the wind speed, the median difference was ~1 m s^{-1} and rarely exceeded 2 m s^{-1}.
2. We proved that the AMPS forecasts can identify the characteristics of atmospheric turbulence over the Antarctic continent in terms of space and time. The R_{xy} of $1/Ri$ at MM, SP, and DC are 0.71, 0.66, and 0.68, respectively, and larger R_{xy} was obtained during warm seasons. Moreover, the value of $1/Ri$ are all underestimated at these three sites. This may be because the model results are generally smoother than the measurements. Furthermore, a model depending on height to improve the AMPS-forecasted $1/Ri$ has been proposed.
3. The seasonal medians of the AMPS forecasts from two vertical cross-sections were presented, and the AMPS forecasts were verified again. it can be observed that the AMPS can forecast the main atmospheric properties as expected: strong temperature inversion near the ground, very calm atmosphere ($1/Ri$ is small) at high altitudes, and a thin boundary layer above the Antarctic Plateau, especially in the summit area. Moreover, we also obtained a new result, that strong wind shears near the escarpment regions have occurred from the ground to ~5 km AGL, causing a thick turbulent atmosphere with large values of $1/Ri$ (or thick boundary layer), which is more evident during the polar winter. In addition, according to the

https://doi.org/10.5194/acp-2022-352
Preprint. Discussion started: 8 November 2022


Atmospheric Chemistry and Physics Discussions

temporal evolution of $1/Ri$ vertical cross-sections for a year from the video supplement, we find that unstable atmospheres are likely to be triggered over the ocean, move toward the Antarctic Plateau, and become stable.

4. The AMPS can forecast the boundary-layer height ($PBLH$). And the $1/Ri$ at the $PBLH$ ($1/Ri_{PBLH}$) was calculated in this study, which could be a helpful reference standard for judging whether the atmospheric layer is stable ($1/Ri < 1/Ri_{PBLH}$) or unstable ($1/Ri > 1/Ri_{PBLH}$) when using AMPS-forecasted $1/Ri$. The median value of $1/Ri_{PBLH}$ from the combined data of two vertical cross-sections is 0.55, which has been used for estimating the $PBLH$ and agrees well with the AMPS-forecasted $PBLH$ (R_{xy} >0.72).

The overall results show that the AMPS can forecast the behaviour of $1/Ri$ and could be applied to practical operations such as astronomy in Antarctica, which is interested in the impacts of atmospheric turbulence (Burton, 2010).

Data availability

The meteorological parameters measured by radiosoundings at McMurdo, South Pole that support the findings of this study are available at the Antarctic Meteorological Research Center (ftp://amrc.ssec.wisc.edu/pub), while the meteorological parameters at Dome C are available at the Antarctic Meteo-Climatological Observatory (http://www.climantartide.it). The original WRF output files of AMPS used in this study can be found at https://www2.mmm.ucar.edu/rt/amps/information/amps_esg_data_info.html.

Video supplement

The video supplement related to the vertical cross-section through the South Pole and Dome C in this article is available online at https://doi.org/10.5446/57377. Another vertical cross-section through Dome A and McMurdo is https://doi.org/10.5446/57378.

Author contributions

QY and XW planned the investigation; QY, XH, and ZW analyzed the data; QY and YG wrote the manuscript draft; QY finished the visualizition; XW, XH, and ZW performed the valiation; XW, CQ, TL, and PW reviewed and edited the manuscript.

Competing interests

The authors declare that they have no conflict of interest.

https://doi.org/10.5194/acp-2022-352
Preprint. Discussion started: 8 November 2022

Atmospheric Chemistry and Physics Discussions

Acknowledgments

This work was supported by the National Natural Science Foundation of China (grant No. 91752103, 41576185) and the Foundation of Advanced Laser Technology Laboratory of Anhui Province (grant No. AHL2021QN02).

References

Agabi, A., Aristidi, E., Azouit, M., Fossat, E., Martin, F., Sadibekova, T., Vernin, J., and Ziad, A.: First Whole Atmosphere Nighttime Seeing Measurements at Dome C, Antarctica, Publications of the Astronomical Society of the Pacific, 118, 344-348, 10.1086/498728, 2006.

Argentini, S., Pietroni, I., Mastrantonio, G., Viola, A. P., Dargaud, G., and Petenko, I.: Observations of near surface wind speed, temperature and radiative budget at Dome C, Antarctic Plateau during 2005, Antarctic Science, 26, 104-112, 10.1017/s0954102013000382, 2013.

Aristidi, E., Agabi, K., Azouit, M., Fossat, E., Vernin, J., Travouillon, T., Lawrence, J. S., Meyer, C., Storey, J. W. V., Halter, B., Roth, W. L., and Walden, V.: An analysis of temperatures and wind speeds above Dome C, Antarctica, Astronomy & Astrophysics, 430, 739-746, 10.1051/0004-6361:20041876, 2005.

Aristidi, E., Vernin, J., Fossat, E., Schmider, F. X., Travouillon, T., Pouzenc, C., Traullé, O., Genthon, C., Agabi, A., Bondoux, E., Challita, Z., Mékarnia, D., Jeanneaux, F., and Bouchez, G.: Monitoring the optical turbulence in the surface layer at Dome C, Antarctica, with sonic anemometers, Monthly Notices of the Royal Astronomical Society, 454, 4304-4315, 10.1093/mnras/stv2273, 2015.

Bonner, C. S., Ashley, M. C. B., Cui, X., Feng, L., Gong, X., Lawrence, J. S., Luong-Van, D. M., Shang, Z., Storey, J. W. V., Wang, L., Yang, H., Yang, J., Zhou, X., and Zhu, Z.: Thickness of the Atmospheric Boundary Layer Above Dome A, Antarctica, during 2009, Publications of the Astronomical Society of the Pacific, 122, 1122-1131, 10.1086/656250, 2010.

Boville, B. A., Kiehl, J. T., and Briegleb, B. P.: Evolution of the Antarctic polar vortex in spring: Response of a GCM to a prescribed Antarctic ozone hole, NASA, Goddard Space Flight Center, Polar Ozone Workshop., N89-14589, 224-227, https://ntrs.nasa.gov/citations/19890005218, 1988.

Bromwich, D. H., Otieno, F. O., Hines, K. M., Manning, K. W., and Shilo, E.: Comprehensive evaluation of polar weather research and forecasting model performance in the Antarctic, Journal of Geophysical Research: Atmospheres, 118, 274-292, 10.1029/2012jd018139, 2013.

Burton, M. G.: Astronomy in Antarctica, Astron. Astrophys. Rev., 18, 417-469, 10.1007/s00159-010-0032-2, 2010.

Chan, P. W.: Determination of Richardson number profile from remote sensing data and its aviation application, IOP Conference Series: Earth and Environmental Science 1, 012043, 10.1088/1755-1307/1/1/012043, 2008.

Gallée, H., Preunkert, S., Argentini, S., Frey, M. M., Genthon, C., Jourdain, B., Pietroni, I., Casasanta, G., Barral, H., Vignon, E., Amory, C., and Legrand, M.: Characterization of the boundary layer at Dome C (East Antarctica) during the OPALE summer campaign, Atmos. Chem. Phys., 15, 6225-6236, 10.5194/acp-15-6225-2015, 2015.

Geissler, K. and Masciadri, E.: Meteorological Parameter Analysis above Dome C Using Data from the European Centre for Medium-Range Weather Forecasts, Publications of the Astronomical Society of the Pacific, 118, 1048-1065, 10.1086/505891, 2006.

Hagelin, S., Masciadri, E., Lascaux, F., and Stoesz, J.: Comparison of the atmosphere above the South Pole, Dome C and Dome A: first attempt, Monthly Notices of the Royal Astronomical Society, 387, 1499-1510, 10.1111/j.1365-2966.2008.13361.x, 2008.

Han, Y., Yang, Q., Liu, N., Zhang, K., Qing, C., Li, X., Wu, X., and Luo, T.: Analysis of wind-speed profiles and optical turbulence above Gaomeigu and the Tibetan Plateau using ERA5 data, Monthly Notices of the Royal Astronomical Society, 501, 4692-4702, 10.1093/mnras/staa2960, 2021.

Hines, K. M. and Bromwich, D. H.: Development and Testing of Polar Weather Research and Forecasting (WRF) Model. Part I: Greenland Ice Sheet Meteorology*, Monthly Weather Review, 136, 1971-1989, 10.1175/2007mwr2112.1, 2008.

Hines, K. M., Bromwich, D. H., Bai, L., Bitz, C. M., Powers, J. G., and Manning, K. W.: Sea Ice Enhancements to Polar WRF*, Monthly Weather Review, 143, 2363-2385, 10.1175/mwr-d-14-00344.1, 2015.

Hines, K. M., Bromwich, D. H., Wang, S.-H., Silber, I., Verlinde, J., and Lubin, D.: Microphysics of summer clouds in central West Antarctica simulated by the Polar Weather Research and Forecasting Model (WRF) and the Antarctic Mesoscale Prediction System (AMPS), Atmospheric Chemistry and Physics, 19, 12431-12454, 10.5194/acp-19-12431-2019, 2019.

Holtslag, A. A. M., de Bruijn, E. I. F., and Pan, H.-L.: A High Resolution Air Mass Transformation Model for Short-Range Weather Forecasting, Monthly Weather Review, 118, 1561, 10.1175/1520-0493(1990)118<1561:Ahramt>2.0.Co;2, 1990.

https://doi.org/10.5194/acp-2022-352
Preprint. Discussion started: 8 November 2022

Atmospheric Chemistry and Physics Discussions

Hu, Y., Hu, K., Shang, Z., Ashley, M. C. B., Ma, B., Du, F., Li, Z., Liu, Q., Wang, W., Yang, S., Yu, C., and Zeng, Z.: Meteorological Data from KLAWS-2G for an Astronomical Site Survey of Dome A, Antarctica, Publications of the Astronomical Society of the Pacific, 131, 015001, 10.1088/1538-3873/aae916, 2019.

Hudson, S. R. and Brandt, R. E.: A Look at the Surface-Based Temperature Inversion on the Antarctic Plateau, Journal of Climate, 18, 1673-1696, 10.1175/jcli3360.1, 2005.

Janjić, Z. I.: The Step-Mountain Eta Coordinate Model: Further Developments of the Convection, Viscous Sublayer, and Turbulence Closure Schemes, Monthly Weather Review, 122, 927-945, 10.1175/1520-0493(1994)122<0927:Tsmecm>2.0.Co;2, 1994.

Karpetchko, A., Kyrö, E., and Knudsen, B. M.: Arctic and Antarctic polar vortices 1957–2002 as seen from the ERA-40 reanalyses, Journal of Geophysical Research, 110, 10.1029/2005jd006113, 2005.

Lascaux, F., Masciadri, E., Hagelin, S., and Stoesz, J.: Mesoscale optical turbulence simulations at Dome C, Monthly Notices of the Royal Astronomical Society, 398, 1093-1104, 10.1111/j.1365-2966.2009.15151.x, 2009.

Listowski, C. and Lachlan-Cope, T.: The microphysics of clouds over the Antarctic Peninsula – Part 2: modelling aspects within Polar WRF, Atmospheric Chemistry and Physics, 17, 10195-10221, 10.5194/acp-17-10195-2017, 2017.

Ma, B., Shang, Z., Hu, Y., Hu, K., Wang, Y., Yang, X., Ashley, M. C. B., Hickson, P., and Jiang, P.: Night-time measurements of astronomical seeing at Dome A in Antarctica, Nature, 583, 771-774, 10.1038/s41586-020-2489-0, 2020.

Ma, Y., Bian, L., Xiao, C., Allison, I., and Zhou, X.: Near surface climate of the traverse route from Zhongshan Station to Dome A, East Antarctica, Antarctic Science, 22, 443-459, 10.1017/s0954102010000209, 2010.

Marks, R. D., Vernin, J., Azouit, M., Manigault, J. F., and Clevelin, C.: Measurement of optical seeing on the high antarctic plateau, Astronomy and Astrophysics Supplement Series, 134, 161-172, 10.1051/aas:1999100, 1999.

Obukhov, A. M.: Turbulence in an atmosphere with a non-uniform temperature, Boundary-Layer Meteorology, 2, 7-29, 10.1007/BF00718085, 1971.

Petenko, I., Argentini, S., Pietroni, I., Viola, A., Mastrantonio, G., Casasanta, G., Aristidi, E., Bouchez, G., Agabi, A., and Bondoux, E.: Observations of optically active turbulence in the planetary boundary layer by sodar at the Concordia astronomical observatory, Dome C, Antarctica, Astronomy & Astrophysics, 568, 10.1051/0004-6361/201323299, 2014.

Pietroni, I., Argentini, S., Petenko, I., and Sozzi, R.: Measurements and Parametrizations of the Atmospheric Boundary-Layer Height at Dome C, Antarctica, Boundary-Layer Meteorology, 143, 189-206, 10.1007/s10546-011-9675-4, 2011.

Powers, J. G., Monaghan, A. J., Cayette, A. M., Bromwich, D. H., Kuo, Y.-H., and Manning, K. W.: Real-Time Mesoscale Modeling Over Antarctica: The Antarctic Mesoscale Prediction System*, Bulletin of the American Meteorological Society, 84, 1533-1545, 10.1175/bams-84-11-1533, 2003.

Rinke, A., Ma, Y., Bian, L., Xin, Y., Dethloff, K., Persson, P. O. G., Lüpkes, C., and Xiao, C.: Evaluation of atmospheric boundary layer-surface process relationships in a regional climate model along an East Antarctic traverse, Journal of Geophysical Research: Atmospheres, 117, n/a-n/a, 10.1029/2011jd016441, 2012.

Seefeldt, M. W., Cassano, J. J., and Nigro, M. A.: A Weather-Pattern-Based Approach to Evaluate the Antarctic Mesoscale Prediction System (AMPS) Forecasts: Comparison to Automatic Weather Station Observations, Weather and Forecasting, 26, 184-198, 10.1175/2010waf2222444.1, 2011.

Swain, Mark R. and Gallée, H.: Antarctic Boundary Layer Seeing, Publications of the Astronomical Society of the Pacific, 118, 1190-1197, 10.1086/507153, 2006.

Town, M. S. and Walden, V. P.: Surface energy budget over the South Pole and turbulent heat fluxes as a function of an empirical bulk Richardson number, Journal of Geophysical Research, 114, 10.1029/2009jd011888, 2009.

Travouillon, T., Ashley, M. C. B., Burton, M. G., Storey, J. W. V., and Loewenstein, R. F.: Atmospheric turbulence at the South Pole and its implications for astronomy, Astronomy & Astrophysics, 400, 1163-1172, 10.1051/0004-6361:20021814, 2003.

Trinquet, H., Agabi, A., Vernin, J., Azouit, M., Aristidi, E., and Fossat, E.: Nighttime Optical Turbulence Vertical Structure above Dome C in Antarctica, Publications of the Astronomical Society of the Pacific, 120, 203-211, 10.1086/528808, 2008.

Troen, I. B. and Mahrt, L.: A simple model of the atmospheric boundary layer; sensitivity to surface evaporation, Boundary-Layer Meteorology, 37, 129-148, 10.1007/BF00122760, 1986.

Vázquez B, G. E. and Grejner-Brzezinska, D. A.: GPS-PWV estimation and validation with radiosonde data and numerical weather prediction model in Antarctica, GPS Solutions, 17, 29-39, 10.1007/s10291-012-0258-8, 2012.

Vernin, J., Chadid, M., Aristidi, E., Agabi, A., Trinquet, H., and Van der Swaelmen, M.: First single star scidar measurements at Dome C, Antarctica, Astronomy & Astrophysics, 500, 1271-1276, 10.1051/0004-6361/200811119, 2009.

Wille, J. D., Bromwich, D. H., Cassano, J. J., Nigro, M. A., Mateling, M. E., and Lazzara, M. A.: Evaluation of the AMPS Boundary Layer Simulations on the Ross Ice Shelf, Antarctica, with Unmanned Aircraft Observations, Journal of Applied Meteorology and Climatology, 56, 2239-2258, 10.1175/jamc-d-16-0339.1, 2017.

Wille, J. D., Bromwich, D. H., Nigro, M. A., Cassano, J. J., Mateling, M., Lazzara, M. A., and Wang, S.-H.: Evaluation of the AMPS Boundary Layer Simulations on the Ross Ice Shelf with Tower Observations, Journal of Applied Meteorology and Climatology, 55, 2349-2367, 10.1175/jamc-d-16-0032.1, 2016.

https://doi.org/10.5194/acp-2022-352
Preprint. Discussion started: 8 November 2022


Atmospheric Chemistry and Physics Discussions

Xie, B., Fung, J. C. H., Chan, A., and Lau, A.: Evaluation of nonlocal and local planetary boundary layer schemes in the WRF model, Journal of Geophysical Research: Atmospheres, 117, n/a-n/a, 10.1029/2011jd017080, 2012.

Yagüe, C., Maqueda, G., and Rees, J. M.: Characteristics of turbulence in the lower atmosphere at Halley IV station, Antarctica, Dynamics of Atmospheres & Oceans, 34, 205-223, 10.1016/S0377-0265(01)00068-9, 2001.

Yang, Q., Wu, X., Han, Y., and Qing, C.: Estimation of behavior of optical turbulence during summer in the surface layer above the Antarctic Plateau using the Polar WRF model, Applied Optics, 60, 4084-4094, 10.1364/ao.419473, 2021a.

Yang, Q., Wu, X., Han, Y., Qing, C., Wu, S., Su, C., Wu, P., Luo, T., and Zhang, S.: Estimating the astronomical seeing above Dome A using Polar WRF based on the Tatarskii equation, Optics Express, 29, 44000-44011, 10.1364/oe.439819, 2021b.

Zuev, V. V. and Savelieva, E.: The cause of the strengthening of the Antarctic polar vortex during October–November periods, Journal of Atmospheric and Solar-Terrestrial Physics, 190, 1-5, 10.1016/j.jastp.2019.04.016, 2019a.

Zuev, V. V. and Savelieva, E.: The cause of the spring strengthening of the Antarctic polar vortex, Dynamics of Atmospheres and Oceans, 87, 10.1016/j.dynatmoce.2019.101097, 2019b.